Environmental Science & Technology

Article

pubs.acs.org/est

Co-Transport of Polycyclic Aromatic Hydrocarbons by Motile Microorganisms Leads to Enhanced Mass Transfer under Diffusive Conditions

Dorothea Gilbert,[†,‡] Hans H. Jakobsen,[§] Anne Winding,[†] and Philipp Mayer*[,†,⊥]

[†]Department of Environmental Science, Aarhus University, P.O. Box 358, 4000 Roskilde, Denmark

[‡]Department of Plant and Environmental Science, University of Gothenburg, Box 462, 405 30 Göteborg, Sweden

[§]Department of Bioscience, Aarhus University, P.O. Box 358, 4000 Roskilde, Denmark

Supporting Information

ABSTRACT: The environmental chemodynamics of hydrophobic organic chemicals (HOCs) are often rate-limited by diffusion in stagnant boundary layers. This study investigated whether motile microorganisms can act as microbial carriers that enhance mass transfer of HOCs through diffusive boundary layers. A new experimental system was developed that allows (1) generation of concentration gradients of HOCs under the microscope, (2) exposure and direct observation of microorganisms in such gradients, and (3) quantification of HOC mass transfer. Silicone O-rings were integrated into a Dunn chemotaxis chamber to serve as sink and source for polycyclic aromatic hydrocarbons (PAHs). This resulted in stable concentration gradients in water (>24 h). Adding the model organism *Tetrahymena pyriformis* to the experimental system enhanced PAH mass transfer up to hundred-fold (benzo[a]pyrene). Increasing mass transfer enhancement with hydrophobicity indicated PAH co-transport with the motile organisms. Fluorescence microscopy confirmed such transport. The effective diffusivity of *T. pyriformis*, determined by video imaging microscopy, was found to exceed molecular diffusivities of the PAHs up to four-fold. Cell-bound PAH fractions were determined to range from 28% (naphthalene) to 92% (pyrene). Motile microorganisms can therefore function as effective carriers for HOCs under diffusive conditions and might significantly enhance mobility and availability of HOCs.

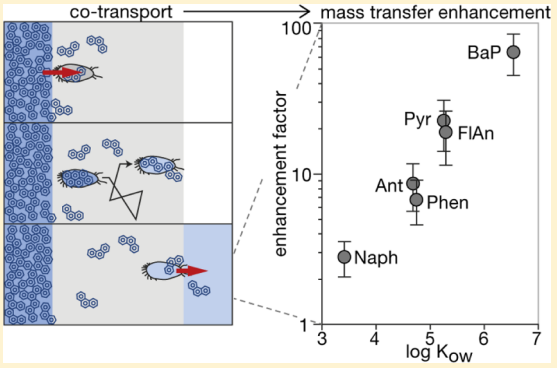

INTRODUCTION

Hydrophobic organic chemicals (HOCs) are widespread contaminants in the environment. The low water solubility of HOCs and their tendency to bind or sorb to immobile organic phases often limit HOC exposure, mobility, transport, and remediation. However, if such organic binding phases are mobile, they can become carrier vehicles and enhance HOC mobility by co-transport.[1] The principle of co-transport can be illustrated with the transport of persistent organic pollutants by for instance migrating birds, fish or whales: (1) Contaminants are taken up at a polluted site, (2) transported with the carrier, and (3) released at a deposition site. Such biotransport has been shown to play a role in the overall contaminant mobility on large spatial scale.[2] Most research, however, has focused on abiotic co-transport with colloids, particles, dissolved organic carbon (DOC), e.g., humic acid, and various molecular carriers.

It is important to distinguish convective and diffusive co-transport, and to pay special attention to the velocity of the carrier relative to the velocity of the unbound contaminants. Convective co-transport has long been recognized as an important transport mechanism for contaminant migration on the macroscale.[3−6] Here the carrier vehicles with the bound molecules are transported together with the aqueous solution they are part of, which implies that bound and unbound forms of the molecules generally move with the same velocity. Significant convective co-transport thus occurs when a significant part of the contaminant is bound to mobile vehicles, a condition that for instance often is given for the leaching of hydrophobic soil pollutants to groundwater and runoff streams. Numerous studies considered colloid-facilitated transport of chemicals in complex transport models[7−10] or investigated experimentally the co-transport of chemicals such as radionuclides,[11,12] heavy metals,[13] and organic chemicals[14] in the subsurface environment. Lindqvist and Enfield[15] were the first to investigate the effect of biocolloids on contaminant transport and indeed found that the convective transport of DDT through sand columns was increased in the presence of bacteria, which the authors attributed to a co-transport mechanism. A similar study with phenanthrene by Jenkins and Lion[16] confirmed such bacteria-facilitated transport.

Received: October 28, 2013
Revised: March 13, 2014
Accepted: March 13, 2014
Published: March 13, 2014

   dx.doi.org/10.1021/es404793u | Environ. Sci. Technol. 2014, 48, 4368−4375

Diffusive co-transport has been demonstrated and reported more recently.[17−24] Here the carrier-bound molecules diffuse in addition to the unbound form, which can lead to enhanced diffusive mass transfer on the microscale. This is especially relevant for mass transfer through stagnant boundary layers that often constitute the bottleneck for the diffusive exchange of HOCs. The carrier vehicle with the bound molecules will always be much larger than the unbound molecule, which has the important implication of lower diffusive velocities of the bound compared to the unbound contaminants. Consequently, significant diffusive co-transport of a contaminant can only occur when the population of carrier-bound molecules markedly exceeds the population of unbound molecules.[20] Diffusive co-transport is thus particularly relevant for the transport of highly hydrophobic chemicals (log K_{ow} > 5) in rather rich media (e.g., digestive fluids).[20]

While co-transport with particles or molecular carriers requires a large contaminant fraction bound to the carrier to be effective, significant co-transport of even small carrier-bound fractions would be possible when the carrier vehicle actively moves faster than the unbound contaminant. The present study was therefore directed at the possible co-transport of PAHs by self-propelled microorganisms. Notably, small organisms increase their diffusivity by orders of magnitude by self-propulsion relative to diffusivities of nonpropelled particles of the same size. This is illustrated in Figure 1 that shows effective diffusion coefficients of self-propelled organisms being orders of magnitude higher compared to aqueous diffusion coefficients of equally sized particles and diffusivities of molecular species. The organisms' effective diffusivities were collected from the literature,[25−28] and their diffusion coefficients were calculated from the reported equivalent spherical diameter using the Stokes−Einstein equation $D = k_b T/6\pi\eta r$. For molecular species, D_{water} was calculated from the regression $D_{water} = 2.7 \times 10^{-4}/M^{0.71}$,[29] where M is the molecular weight.

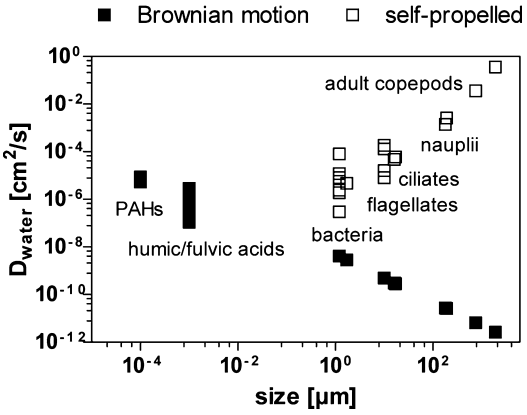

Figure 1. Small organisms increase their diffusivity by orders of magnitude by self-propulsion and could act as an effective transport vector for hydrophobic organic chemicals such as PAHs.

The aim of this study was to investigate with the ciliate *Tetrahymena pyriformis* as model organism to what extent microbial co-transport can enhance the transport of HOCs under diffusive conditions. PAHs were chosen as model chemicals to cover a range of physicochemical properties of HOCs.

Working Principle. A Dunn chemotaxis chamber[30] was employed into which two silicone O-rings were integrated to serve as a partitioning source and sink for hydrophobic chemicals (Figure 2). The chamber consists of an inner and outer annular well on a glass slide between which a small gap over a glass bridge allows for diffusive exchange. The smaller silicone ring is loaded with a test chemical and placed into the inner well, whereas the larger silicone ring is left clean and placed into the outer well. Aqueous medium is added and the chamber is closed with a coverslip. Partitioning of the chemical between silicone and the aqueous medium then controls the concentrations in the wells,[31] which results in a stable linear concentration gradient over the bridge. This allows exposure of microorganisms to defined concentration gradients and their direct observation by microscopy. At the end of the experiment, both silicone rings can be extracted and the measured concentrations then be used to deduce the diffusive flux over the bridge.

MATERIALS AND METHODS

Diffusion Model for PAH Transfer in the Dunn Chamber. Diffusive mass transfer of PAHs in the Dunn chamber can be described by the linear differential equation

$$\frac{dm_o(t)}{dt} = -\frac{dm_i(t)}{dt} = k_i m_i(t) - k_o m_o(t) \quad (1)$$

where m_o [g] is the mass of analyte recovered in the outer ring (sink), m_i the mass of analyte in the inner ring (source), and where k_i and k_o [s^{-1}] denote the velocity rate constants for the mass transfer from the inner to the outer ring and from the

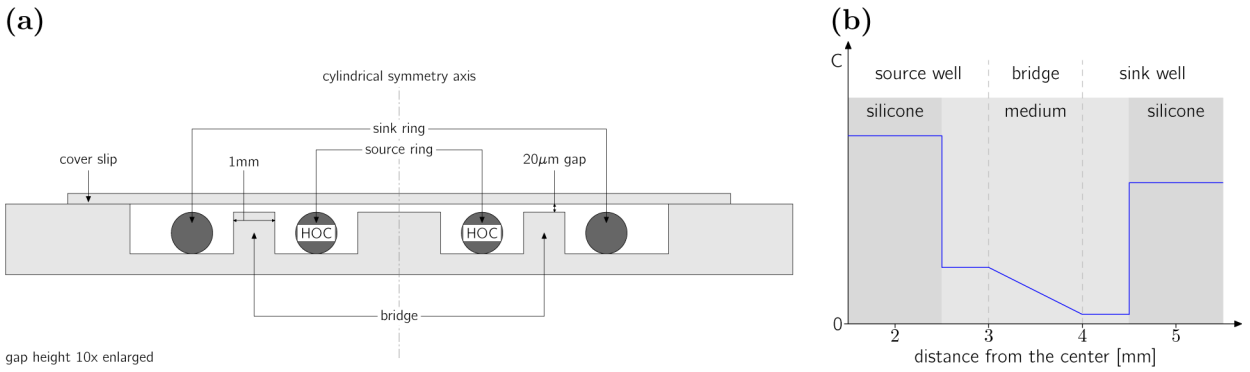

Figure 2. (a) Cross-section of a Dunn chamber with silicone O-rings. (b) Schematic concentration profile from source to sink illustrating the working principle: hydrophobic organic chemicals (HOC) partition between silicone and medium and form a diffusive concentration gradient over the glass bridge between the wells.

dx.doi.org/10.1021/es404793u | Environ. Sci. Technol. 2014, 48, 4368−4375

outer to the inner ring, respectively. With the total analyte mass (m_{tot}) given by

$$m_o(t) + m_i(t) = m_{tot} \quad (2)$$

and the initial condition $m_o(t = 0) = 0$, the solution to the differential equation is given as

$$m_o(t) = m_{tot}\frac{k_i}{k_i + k_o}(1 - e^{-(k_i+k_o)t}) \quad (3)$$

under the assumption that all mass released from the source is recovered in the sink and $m_{tot} = m_i(t = 0)$ at any time. Equilibrium is reached when the analyte concentration in the inner ring equals that in the outer ring: $C_i = C_o$ or with C as mass divided by volume (V)

$$\frac{m_i(t = \infty)}{V_i} = \frac{m_o(t = \infty)}{V_o} \quad (4)$$

Considering that at equilibrium $dm_o(t)/dt = 0$, and by substituting eq 4 into eq 2, we obtain eq 5 as equilibrium criterion.

$$\frac{m_o(t = \infty)}{m_{tot}} = \frac{k_i}{k_i + k_o} = \frac{V_o}{V_o + V_i} \quad (5)$$

Hence, eq 3 can be rewritten as

$$\frac{m_o(t)}{m_{tot}} = \frac{V_o}{V_o + V_i}(1 - e^{-kt}) \quad (6)$$

with $k_i + k_o = k$. This equation was used to determine k from experimentally determined ratios of m_o/m_{tot}.

The precise dimensions of the Dunn chamber allow to also predict the rate constants for the diffusive mass transfer from Fick's First law of diffusion:

$$\frac{dC_o(t)}{dt} = D\frac{A}{V_o}\cdot\frac{C_i - C_o}{\Delta x} \quad (7)$$

where $dC_o(t)/dt$ denotes the diffusive flux [$gL^{-1}s^{-1}$] as a function of time into the outer ring, A the surface area [m^2] for diffusive exchange and V_o the volume of the diffusion sink [m^3], D the molecular diffusion coefficient [m^2s^{-1}], and Δx the diffusion path length [m]. Taking into consideration that the capacity of the silicone is by the factor of the partition coefficient $K_{silicone:med}$ larger than that of the medium where diffusion occurs, the rate constant k for the diffusive mass transfer can be predicted from eq 8.

$$k = \left(\frac{1}{V_o} + \frac{1}{V_i}\right)\frac{A\cdot D}{K_{silicone:med}\Delta x} \quad (8)$$

The volumes of source and sink were approximated by calculating the volumes of the silicone rings as $V_i = 9.90 \times 10^{-9}m^3$ and $V_o = 2.47 \times 10^{-8}m^3$. The area for diffusive exchange was calculated from the circumference at the center of the bridge ($r = 3.5$ mm) and the given gap height of 20 μm, yielding $A = 4.40 \times 10^{-7}m^2$. The diffusion path length is given as the width of the bridge $\Delta x = 1$ mm. These values were inserted into eq 8 together with the silicone:water partition coefficients and diffusion coefficients of PAHs in water that are listed in Table S1 in the Supporting Information (SI).

Diffusive Co-transport. In a diffusive co-transport scenario, both the free and the carrier-bound chemical species contribute to the overall mass transfer. While the transport of the free chemical species attributes to molecular diffusion, the transport of carrier-bound species is determined by the diffusivity of the loaded carrier. Mass transfer enhancement factors (EF) for co-transport can be estimated from the ratio of the diffusion coefficients and the distribution ratio of carrier-bound and free chemical (eq 9) under the assumption that the carrier-bound chemical species is in fast equilibrium with the freely dissolved species, i.e. that binding kinetics are not rate-limiting the co-transport:

$$EF = \frac{D_{bound}\cdot bf}{D_{free}\cdot ff} + 1 = \frac{D_{bound}}{D_{free}}\cdot K_{carrier}\cdot[carrier] + 1 \quad (9)$$

with bf being the bound fraction and ff being the free fraction of chemical, which both relate to the binding constant $K_{carrier}$ (carrier:water partition ratio) at a given carrier abundance [carrier], here the cell density. To experimentally derive enhancement factors in this study, the velocity rate constants for the PAH mass transfer through the cell suspension (k_{susp}) and aqueous medium only (k_{med}) were determined, assuming that k_{med} is representative for the velocity rate constants of freely dissolved molecules k_{free}:

$$EF = \frac{k_{susp}}{k_{med}} \approx \frac{k_{bound} + k_{free}}{k_{free}} \quad (10)$$

Chemicals and Materials. The PAHs naphthalene (>99%, Sigma, Germany), anthracene (99%, Acros, Belgium), phenanthrene (98%, Acros), fluoranthene (99%, Aldrich, Germany), pyrene (>99%, Fluka, Germany) and benzo[a]pyrene (98%, Cerilliant, TX) were chosen as model chemicals. Physicochemical properties of these PAHs are provided in SI Table S1. Perylene (>99.5%, Aldrich) was used for fluorescence microscopy. Methanol (HPLC-grade, Merck, Germany) and ultrapure water (Millipore, MA) were used. Silicone O-rings with an inner diameter of 3.0 mm and 9.0 mm and a cross section of 1.0 mm were purchased from Altecweb, UK, (ord.-no. ORS-3x1 and ORS-9x1) and custom-made Dunn chambers with an inner and outer well depth of 1.10 ± 0.05 mm were kindly provided by Hawksley & Sons Ltd., UK.

Tetrahymena pyriformis. The ciliate *Tetrahymena pyriformis* (ATCC strain 30005) was chosen as model organism as it is capable of moving through aqueous media by self-propulsion. The organisms were grown in axenic culture in a proteose peptone medium (ATCC medium 357). Five gram proteose peptone (Difco), 5 g tryptone and 0.2 g K_2HPO_4 were dissolved in 1 L distilled water and the pH was adjusted to 7.2. The culture was kept at 15 °C for long-term storage and an aliquot was transferred to new medium once a month. Subcultures were prepared 48 h prior to the experiments and were kept at room temperature in darkness. The cell density at the beginning of each experiment ranged from 1×10^5 cells mL^{-1} to 5×10^5 cells mL^{-1}.

Mass Transfer Experiments. All silicone rings were cleaned in methanol three times overnight. Small silicone rings were then loaded with a mixture of naphthalene, anthracene, phenanthrene, fluoranthene, pyrene, and benzo[a]pyrene by equilibrium partitioning of the chemicals from a 60:40% v/v methanol:water loading solution.[20,32] The loading solution volume was chosen hundred-fold larger than the silicone volume, and the rings were loaded twice for at least 72 h at room temperature to ensure negligible depletion of the loading solution (details in SI). O-rings were removed from the loading solution and washed three times with a small amount of

water to remove any adhering loading solution before usage. Rings that were to be used as sink were washed with water after the methanol cleaning. Chemical analysis confirmed that PAHs could not be detected in such cleaned rings. For chamber assembly, the protocol by Zicha et al.[30] was modified such that the cell suspension or aqueous medium was first filled into the inner well and a cover glass then moved until centered while the outer well was being filled (details in SI). Thick coverslips (22 mm × 25 mm × 0.5 mm) were used to reduce the variation in gap height.[33] Assembly usually took less than 5 min. At the end of each experiment, the rings were wiped clean with lint-free tissue and were then extracted with 10 mL (source) or 200 μL (sink) of methanol. The minimal extraction volume for an exhaustive extraction had been calculated based on reported methanol:water partition coefficients for PAHs.[31] Methanol was chosen as extraction solvent as it causes limited swelling of the silicone polymer.[34] The mass of each PAH recovered in the outer ring (m_o) at time t [h] was expressed as a fraction of the total mass m_{tot} and the rate constant k was calculated from eq 6.

In a first experiment, the diffusive mass transfer of PAHs through air and water was quantified. Triplicate chambers were assembled and filled with water or without any aqueous solution (diffusion through air) and sampled after 120 h. A second experiment was conducted to test whether motile organisms in the chamber would enhance the mass transfer of PAHs: three chambers were filled with the cell suspension and three chambers with the cell culture medium as controls. Because of the low transfer rates of benzo[a]pyrene, chambers with medium only were let to stand for 120 h whereas chambers with the ciliates were sampled after 24 h when motility of the organisms ceased. Before disassembly, viability of *T. pyriformis* was verified microscopically (Olympus CKX41 inverted microscope, 10× magnification). All experiments were repeated twice on different dates with a blocked experimental design to eliminate bias by differences in the chambers. In an additional experiment, all six chambers were assembled with fluoranthene-loaded rings and let to stand for 24 h to confirm that the mass fraction transferred to the sink (through culture medium) was similar in all chambers (CV = 9.8%).

For confirmation of a complete mass balance, three source rings from the batch to be used were extracted in methanol before starting each experiment to yield the initial mass of analyte ($m_i(t = 0)$). Recovery was then calculated as

$$\text{recovery} = m_{tot}/m_i(t = 0) \tag{11}$$

with m_{tot} being the total analyte mass (eq 2).

Determination of *T. pyriformis*' Diffusivity. In a separate experiment, *T. pyriformis* was exposed to naphthalene gradients in the Dunn chamber and in a control chamber with clean silicone rings, and observed by video imaging microscopy. Because *T. pyriformis* exhibits phototaxis,[35,36] we replaced the light source of the Olympus CKX41 inverted microscope with an infrared LED and recorded videos in darkness (details in SI). Videos were recorded immediately after chamber assembly with a delay of no more than 10 min. The automated cell tracking software LabTrack (vers. 2.3, BioRAS, Denmark) was then used to track the recorded swimming paths of *T. pyriformis*, which yielded *x*-*y*-coordinates over time for each individual cell. Data were analyzed with the software "Chemotaxis and Migration Tool" (ibidi, Germany) to investigate for any directionality in movement of *T. pyriformis* (details in SI). To finally determine the effective diffusivity of *T. pyriformis*, the root-mean-square net displacement RMS [cm] of at least 25 individuals was calculated for each time step Δt [s], and a nonlinear regression by least-squares was performed to fit the data to Taylor's model for diffusion by continuous movements [37]

$$\text{RMS} = [2Dn(\Delta t - \tau(1 - e^{-\Delta t/\tau}))]^{0.5} \tag{12}$$

where n defines the dimensionality (here $n = 2$), τ the time scale for which there is persistence in directionality [s], and D [cm^2s^{-1}] the effective diffusion coefficient.

Fluorescence Microscopy. To visualize the co-transport of PAHs, *T. pyriformis* was exposed to a fluoranthene gradient in the Dunn chamber and observed under a Zeiss Axioplan epifluorescence microscope equipped with a HBO 50W mercury lamp and fluorescence filter sets for excitation and emission at 365/420 nm and 436/470 nm. Fluoranthene was also used to visualize the gradient over the bridge (details in SI). However, UV-light and fluoranthene (at 5% of the solubility limit) in combination caused severe toxicity in *T. pyriformis* and cell death within a few minutes. Therefore, the 5-ring PAH perylene (excitation at 436 nm) was selected for fluorescence microscopy with the ciliates, and O-rings were loaded to saturation. Videos were recorded with a digital camcorder (Canon Legria HF21) that was mounted onto the photoport of the microscope using a special adapter (ord.-no. MM99−58, Martin Microscopes, Easley, SC). A 10× objective and the optical zoom of the camcorder were used for optimal magnification.

Determination of PAH Binding to *T. pyriformis*. To determine PAH binding constants for *T. pyriformis*, a recently developed analytical passive dosing method was employed.[38,39] The method is based on equilibrium partitioning of analytes between a dominating reservoir (silicone) and an aqueous solution or suspension. Briefly, 500 mg of silicone was casted into the bottom of 10 mL glass vials, loaded with a mixture of naphthalene, phenanthrene, anthracene, fluoranthene, and pyrene.[39] *T. pyriformis* was grown to a dense culture (ca. 3.2 × 10^5cells mL^{-1}) at room temperature for 48 h prior to the binding experiments. The loaded silicone vials were then sequentially equilibrated with 2 mL of either water, the cell suspension, or ATCC medium ($n = 3$) in the order water-suspension-water-medium-water at 1000 rpm at room temperature. After equilibration, an aliquot of each sample was taken and methanol added for dissolution of the PAHs from the matrix and subsequent HPLC analysis (see below). The cell-bound fraction (CBF) of PAHs was then calculated as

$$\text{CBF} = \frac{C_{susp(eq)} - C_{med(eq)}}{C_{susp(eq)}} \tag{13}$$

with $C_{susp(eq)}$ being the total concentration in the equilibrated cell suspension and $C_{med(eq)}$ the concentration in the equilibrated culture medium. The free fraction in the cell suspension ff_{susp} was calculated as

$$ff_{susp} = \frac{C_{water(eq)}}{C_{susp(eq)}} \tag{14}$$

with $C_{water(eq)}$ being the equilibrium concentration in pure water. Binding constants for PAHs to *T. pyriformis* ($K_{Tetrahymena}$) were estimated as

$$K_{Tetrahymena} = \frac{C_{susp(eq)} - C_{med(eq)}}{C_{water(eq)}[\text{CD}]} \tag{15}$$

dx.doi.org/10.1021/es404793u | *Environ. Sci. Technol.* 2014, 48, 4368−4375

with [CD] as the cell density of *T. pyriformis*. To convert measured cell densities [cells mL^{-1}] to units of LL^{-1}, the mean cell volume was estimated to 4511 μm^3 from the measured average equivalent spherical diameter of the cells (20.5 μm; Coulter Counter estimate).

Chemical Analysis. Methanol extracts of the silicone rings and aqueous samples from the binding experiment were analyzed by HPLC (Agilent 1100 HPLC) equipped with a multiwavelength fluorescence detector (G1321A FLD). The excitation wavelength was set to 260 nm and PAHs were detected at emission wavelengths of 350, 420, 440, and 500 nm. A volume of 30 μL was injected onto a CP-Ecospher 4 PAH column (Varian Inc., Palo Alto, CA) at 28 °C and PAHs were separated by gradient elution (flow rate of 0.5 mL min^{-1}), starting with a 50:50% v/v mixture of methanol and water (12 min). A two-step linear gradient of 50−75% methanol (5 min) and 75−100% methanol (28 min) was then used and finally 100% methanol (15 min) for elution. Chromatograms were analyzed with the HP Chemstation software (vers. B.03.01, Agilent Technologies, Palo Alto, CA), using a nine-point external calibration line.

RESULTS

Partitioning-Controlled Microgradients. A PAH-loaded and a clean silicone ring were placed in the Dunn chamber to generate a concentration gradient. The concentration in source and sink well was thus controlled by partitioning of the chemicals between the silicone and the medium. The resulting concentration difference between the source well and sink well then led to a linear concentration gradient over the glass bridge, which acted as bottleneck for diffusion between the wells.[30] Finally, fluorescence microscopy with fluoranthene as model PAH was applied to roughly capture and confirm the linear concentration gradient (Figures S1 and S2 in SI).

The gradients remained highly stable in water: the mass fraction (m_o/m_{tot}) transferred after 24 h was 0.685%, 0.056%, 0.042%, 0.018%, 0.016% and 0.002% on average (n = 3) for naphthalene, phenanthrene, anthracene, fluoranthene, pyrene, and benzo[a]pyrene respectively, calculated from the determined velocity rate constants (eq 6), which was in good agreement with the model predictions from Fick's First law of diffusion (Figure 3). Through air, PAH mass transfer was faster with corresponding fractions transferred of 35.0%, 1.268%, 1.061%, 0.154%, 0.130%, and 0.003%. Note that equilibrium is reached only when 71% of the total analyte mass is recovered in the sink. A plot of log-transformed mass transfer rates against the log K_{ow} of the PAHs (Figure S3 in SI) and linear regression yielded a steeper slope and a higher intercept for air (y = $-1.38x + 3.19$, R^2 = 0.97) than for water ($y = 0.81x-0.72$, R^2 = 0.95), confirming earlier findings that the mass transfer of the less hydrophobic PAHs is more effective through air than through water.[20] For all tested PAHs but naphthalene, a mass balance (eq 11) yielded values between 95% and 110% (for naphthalene in air 65% and 79% in water), showing that the assumption of complete recoveries was largely fulfilled (recoveries are reported in Table S3 in SI).

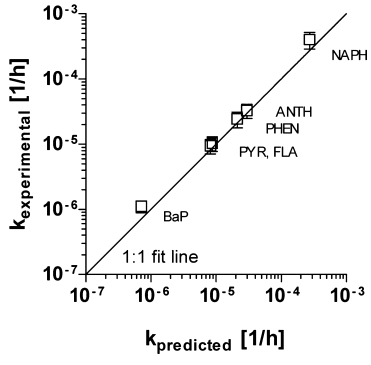

Figure 3. Predicted versus experimental velocity rate constants k for the diffusive mass transfer of PAHs through water with the mean and the standard error of the mean (n = 3) indicated.

Enhanced PAH Transfer by Co-transport with *T. pyriformis*. Mass transfer experiments with the ciliate *T. pyriformis* revealed that PAH transfer was enhanced in the presence of the organisms: PAH transfer was larger in chambers with *T. pyriformis* compared to chambers without the ciliates (Figure 4a and Table S2 in SI). Enhancement factors (eq 10)

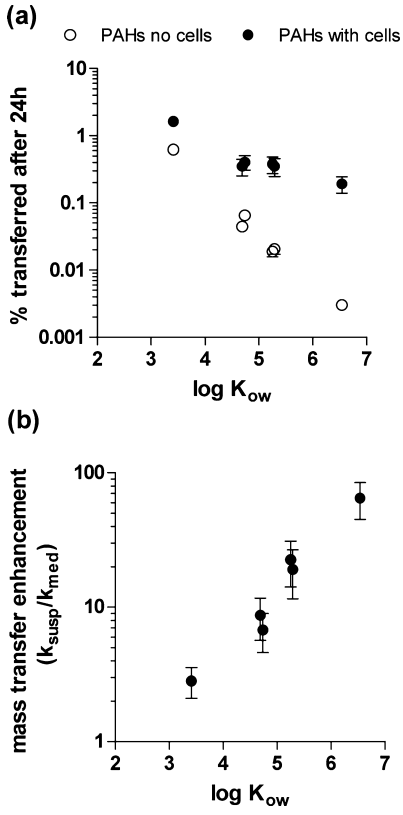

Figure 4. (a) Mass fraction of six PAHs transferred to the sink (m_o/m_{tot}) after 24 h in the presence and absence of *T. pyriformis* and (b) enhancement factors plotted against the octanol−water partition coefficient K_{ow} of the PAHs. Symbols show the mean and the standard error of the mean of three independent experiments, with each experiment performed in triplicate.

increased with increasing hydrophobicity of the PAHs (Figure 4b) from minimal 1.60 ± 0.19 (average and SD for naphthalene) to an average maximal 95.80 ± 11.05 (average and SD for benzo[a]pyrene). Mass transfer rates (eq 6) through aqueous medium decreased with increasing hydrophobicity of the PAHs by three orders of magnitude. In presence of *T. pyriformis*, however, the velocity rate constants for the mass transfer of the six PAHs spanned only over one order of magnitude, indicating that the dominating mass transfer process was not any longer governed by molecular

dx.doi.org/10.1021/es404793u | *Environ. Sci. Technol.* 2014, 48, 4368−4375

diffusion through aqueous medium. This is characteristic for a co-transport mechanism,[20] which in the present experiments only can be attributed to the mobile ciliates functioning as a transport vector for the PAHs.

Using fluorescence microscopy, we were able to directly observe transport and release of perylene by *T. pyriformis*. Organisms that had taken up perylene in vicinity of the loaded silicone ring appeared strongly blue (Figure S5 in SI) and their trajectories could be followed from the fluorescence signal (a video is provided in SI). They became transparent when remaining for a few minutes close to the sink ring and could then only be observed when in addition a bright-field or dark-field illumination was used. The videos also showed that *T. pyriformis* could transport this highly hydrophobic substance within only a few seconds from source to sink. For comparison: the typical time needed for PAHs to travel across a 1 mm distance by molecular diffusion is $t_d = x^2/2D$ with x being the diffusion length and D being the molecular diffusion coefficient and ranges from 9.7 min (naphthalene) to 15.7 min (benzo[a]pyrene).

Diffusivity of *T. pyriformis*. *T. pyriformis* moved frequently between the source and sink well of the Dunn chamber. None of the statistical parameters used to evaluate directionality in movements of *T. pyriformis* indicated chemotactic behavior of the organisms (Table S4 in SI) when exposed to a naphthalene gradients, similar as in the control treatment with clean silicone rings. The center of mass remained close to the origin and the average net displacement length equaled only one to two times the average cell length of *T. pyriformis*. Forward migration indices (FMI) were in both x- and y-direction close to zero and did not indicate any directionality in movement. The Rayleigh test, although not a direct measure for chemotaxis, was performed considering cell end points and did not show a significant nonhomogeneous distribution of cells ($p > 0.05$). Trajectories of *T. pyriformis* when drawn as to start from the origin in a Cartesian coordinate system showed a pattern of random walk (data not shown). This was also confirmed by plotting the computed net length distance traveled by *T. pyriformis* against time: the data obeyed the square root dependence on time that is predicted for diffusing particles in suspension by Taylor's model (eq 12). A nonlinear regression using the Taylor model yielded an effective diffusion coefficient for *T. pyriformis* of $D = 2.2 \times 10^{-5}\mathrm{cm^2s^{-1}}$, which is the average of exposed and nonexposed organisms (regression parameters are given in Table S5 in SI) . This value is in good agreement with the diffusion coefficient reported for another ciliate (*Balanion comatum*; $D = 4.7 \times 10^{-5}\mathrm{cm^2s^{-1}}$) of similar size.[25] Compared to the diffusion coefficients of the PAHs in water, the effective diffusion coefficient of *T. pyriformis*, which in fact is the effective diffusion coefficient of the cell-bound PAHs, is larger by a factor of 2.6 (naphthalene) to 4.1 (benzo[a]pyrene).

PAH Binding to *T. pyriformis*. PAH binding to *T. pyriformis* increased with increasing hydrophobicity of the chemicals. The cell-bound fraction was 28%, 74%, 73%, 89%, and 92% for naphthalene, phenanthrene, anthracene, fluoranthene, and pyrene at a cell density of 3.2×10^5 cells $\mathrm{mL^{-1}}$, which is comparable to cell densities used in the mass transfer experiments. Corresponding free fractions in the cell suspension were 59%, 19%, 16%, 8%, and 6%, respectively. Binding constants were estimated from these data for naphthalene, phenanthrene, anthracene, fluoranthene, and pyrene and amounted to 3.3×10^2, 2.7×10^3, 3.1×10^3, 7.8×10^3, 11.4×10^3 $\mathrm{LL^{-1}}$. They could explain higher mass transfer enhancement factors for the more hydrophobic PAHs: the binding constants inserted into eq 9 together with the determined effective diffusivity of *T. pyriformis* predicted enhancement factors that were in good agreement with the observations for naphthalene. For phenanthrene, anthracene, fluoranthene and pyrene enhancement factors were approximately by a factor of two lower than modeled (Figure S4 in SI), which may be due to kinetic limitations for the uptake and release of PAHs by the organisms.

***T. pyriformis* as Carrier for PAHs.** Since *T. pyriformis* can bind significant amounts of PAHs and because its effective diffusivity is larger than diffusivities of PAHs, it appears to be an efficient transport vehicle for PAHs. Notably, the mass of PAH transferred to the sink by the ciliates over the period of the experiment was approximately two orders of magnitude larger than the estimated amount of PAH the organisms can bind, which implies that *T. pyriformis* crossed the glass bridge between source and sink in the Dunn chamber repeatedly. This suggests that motile microorganisms can function multiple times as transport vehicles and may thus transport fairly large amounts of HOCs when transport is limited to diffusion.

DISCUSSION

Microbial Transport of HOCs. The results of the present study provide experimental evidence that ciliated protozoa can function as fast transport vehicles for hydrophobic organic chemicals. Hence, one may expect that generally any motile microorganisms could act as a shuttle for HOCs, particularly when the effective diffusivities of the microorganisms exceed molecular diffusivities of HOCs (Figure 1). The unique adaptation of microorganisms to move by self-propulsion through aqueous medium makes them effective carriers for HOCs in diffusive boundary layers. Even when only a small fraction of a hydrophobic chemical is bound to a microbial carrier, co-transport with motile microorganisms can significantly enhance the mass transfer of HOCs when transport is diffusion-limited. A recent study by Furuno et al.[40] demonstrated that also fungal mycelial networks (hyphal pipelines) can enhance the mobility of HOCs by actively transporting HOC-containing lipid vesicles within the hyphae. The transport of PAHs through such hyphal pipelines was shown to be much faster than the diffusive transport through aqueous media, and it was also demonstrated that this increased the biodegradation of PAHs.[41] There is thus increasing body of evidence that microorganisms beyond their well-known role as contaminant degraders also play an important role in transporting and distributing contaminants.

Relevance and Implications. Co-transport is especially important for the mass transfer of the more hydrophobic chemicals because only a small mass of those can be accommodated and transported in aqueous medium due to their low aqueous solubilities and high chance for immobilization by sorption and binding to solid phases. The present findings reveal that microbial co-transport of chemicals can play a major role when the transport of HOCs is diffusion-limited, which has important implications for, e.g., the uptake of PAHs into plant roots, their partitioning into biomembranes, or their uptake into passive samplers. It is expected to be a significant if not the dominating transport process relative to the diffusive mass transfer of unbound and DOC-bound HOCs because effective diffusivities of small organisms like bacteria and protozoa can be up to hundred-fold larger than the diffusivities of HOCs and DOC (Figure 1). The transport of HOCs, for

example through soil, may thus be much faster than predictions of present diffusion models would suggest. This emphasizes the importance to incorporate effective diffusivities of microorganisms into contaminant transfer models. The high abundance and mobility of microorganisms in virtually all environmental compartments makes microbial co-transport a transport process that may affect various chemodynamic processes in the environment: Microbial co-transport may accelerate biological uptake, which may modify toxic responses or bioaccumulation rates. Further, it contributes to the mobilization of hydrophobic organic pollutants by accelerating desorption from soil or sediment, and hence increases contaminant mobility and mixing. This in turn could accelerate the transfer of HOCs to degrading organisms and hence biodegradation, which may find application in the bioremediation of HOC-polluted sites.

■ ASSOCIATED CONTENT

Supporting Information

Included is a complete description of the material and methods, a plot of the velocity rate constants for the PAH mass transfer through air and water as a function of log K_{ow}, recoveries and PAH measurements from the mass transfer experiments, as well as the statistical evaluation of directionality in movement and the regression parameters for the Taylor-fit. Fluorescence images are shown visualizing the concentration gradient in the Dunn chamber. Also available is a fluorescence microscopy video showing the co-transport of perylene with *T. pyriformis*. This material is available free of charge via the Internet at http://pubs.acs.org/.

■ AUTHOR INFORMATION

Corresponding Author

*Phone: +45 4525 1569; e-mail: philm@env.dtu.dk.

Present Address

[⊥](P.M.) Department of Environmental Engineering, Technical University of Denmark, 2800 Kgs. Lyngby, Denmark.

Notes

The authors declare no competing financial interest.

■ ACKNOWLEDGMENTS

We thank Hawksley & Sons Ltd. for providing modified Dunn chambers and BioRAS for providing access to the LabTrack software. Jeppe Lund Nielsen is thanked for help with microscopy, and Thomas Backhaus is acknowledged as co-supervisor during the project. Financial support was given through the OSIRIS and MODELPROBE projects and a scholar stipend from the Research School of Environmental Chemistry and Toxicology (RECETO).

■ REFERENCES

(1) McCarthy, J. F.; Zachara, J. M. Subsurface transport of contaminants. *Environ. Sci. Technol.* **1989**, *23*, 496−502.

(2) Blais, J. M.; Macdonald, R. W.; Mackay, D.; Webster, E.; Harvey, C.; Smol, J. P. Biologically mediated transport of contaminants to aquatic systems. *Environ. Sci. Technol.* **2007**, *41*, 1075−1084.

(3) Magee, B. R.; Lion, L. W.; Lemley, A. T. Transport of dissolved organic macromolecules and their effect on the transport of phenanthrene in porous media. *Environ. Sci. Technol.* **1991**, *25*, 323−331.

(4) Dunnivant, F. M.; Jardine, P. M.; Taylor, D. L.; McCarthy, J. F. Co-transport of cadmium and hexachlorobiphenyl by dissolved organic carbon through columns containing aquifer material. *Environ. Sci. Technol.* **1992**, *26*, 360−368.

(5) Newman, M. E.; Elzerman, A. W.; Looney, B. B. Facilitated transport of selected metals in aquifer material packed columns. *J. Contam. Hydrol.* **1993**, *14*, 233−246.

(6) Corapcioglu, M. Y.; Kim, S. H. Modeling facilitated contaminant transport by mobile bacteria. *Water Resour. Res.* **1995**, *31*, 2639−2647.

(7) Johnson, W. P.; Amy, G. L. Facilitated transport and enhanced desorption of polycyclic aromatic-hydrocarbons by natural organic-matter in aquifer sediments. *Environ. Sci. Technol.* **1995**, *29*, 807−817.

(8) Kim, S. B.; Corapcioglu, M. Y.; Kim, D. J. Effect of dissolved organic matter and bacteria on contaminant transport in riverbank filtration. *J. Contam. Hydrol.* **2003**, *66*, 1−23.

(9) Saiers, J. E.; Hornberger, G. M. Modeling bacteria-facilitated transport of DDT. *Water Resour. Res.* **1996**, *32*, 1455−1459.

(10) Simunek, J.; He, C.; Pang, L.; Bradford, S. A. Colloid-facilitated solute transport in variably saturated porous media: Numerical model and experimental verification. *Vadose Zone J.* **2006**, *5*, 1035−1047.

(11) Artinger, R.; Rabung, T.; Kim, J.; Sachs, S.; Schmeide, K.; Heise, K.; Bernhard, G.; Nitsche, H. Humic colloid-borne migration of uranium in sand columns. *J. Contam. Hydrol.* **2002**, *58*, 1−12.

(12) Mibus, J.; Sachs, S.; Pfingsten, W.; Nebelung, C.; Bernhard, G. Migration of uranium(IV)/(VI) in the presence of humic acids in quartz sand: A laboratory column study. *J. Contam. Hydrol.* **2007**, *89*, 199−217.

(13) Pang, L.; Close, M. E.; Noonan, M. J.; Flintoft, M. J.; van den Brink, P. A laboratory study of bacteria-facilitated cadmium transport in alluvial gravel aquifer media. *J. Environ. Qual.* **2005**, *34*, 237−247.

(14) Villholth, K. G.; Jarvis, N. J.; Jacobsen, O. H.; de Jonge, H. Field investigations and modeling of particle-facilitated pesticide transport in macroporous soil. *J. Environ. Qual.* **2000**, *29*, 1298−1309.

(15) Lindqvist, R.; Enfield, C. G. Biosorption of dichlorodiphenyltrichloroethane and hexachlorobenzene in groundwater and its implications for facilitated transport. *Appl. Environ. Microbiol.* **1992**, *58*, 2211−2218.

(16) Jenkins, M. B.; Lion, L. W. Mobile bacteria and transport of polynuclear aromatic-hydrocarbons in porous media. *Appl. Environ. Microbiol.* **1993**, *59*, 3306−3313.

(17) Kopinke, F.-D.; Georgi, A.; Mackenzie, K. Sorption and chemical reactions of PAHs with dissolved humic substances and related model polymers. *Acta Hydrochim. Hydrobiol.* **2000**, *28*, 385−399.

(18) Oomen, A. G.; Mayer, P.; Tolls, J. Nonequilibrium solid phase microextraction for determination of the freely dissolved concentration of hydrophobic organic compounds: Matrix effects and limitations. *Anal. Chem.* **2000**, *72*, 2802−2808.

(19) Mayer, P.; Karlson, U.; Christensen, P. S.; Johnsen, A. R.; Trapp, S. Quantifying the effect of medium composition on the diffusive mass transfer of hydrophobic organic chemicals through unstirred boundary layers. *Environ. Sci. Technol.* **2005**, *39*, 6123−6129.

(20) Mayer, P.; Fernqvist, M. M.; Christensen, P. S.; Karlson, U.; Trapp, S. Enhanced diffusion of polycyclic aromatic hydrocarbons in artificial and natural aqueous solutions. *Environ. Sci. Technol.* **2007**, *41*, 6148−6155.

(21) Kramer, N. I.; van Eijkeren, J. C. H.; Hermens, J. L. M. Influence of albumin on sorption kinetics in solid-phase microextraction: Consequences for chemical analyses and uptake processes. *Anal. Chem.* **2007**, *79*, 6941−6948.

(22) Haftka, J. J. H.; Parsons, J. R.; Govers, H. A. J.; Ortega-Calvo, J.-J. Enhanced kinetics of solid-phase microextraction and biodegradation of polycyclic aromatic hydrocarbons in the presence of dissolved organic matter. *Environ. Toxicol. Chem.* **2008**, *27*, 1526−1532.

(23) ter Laak, T. L.; van Eijkeren, J. C. H.; Busser, F. J. M.; van Leeuwen, H. P.; Hermens, J. L. M. Facilitated transport of polychlorinated biphenyls and polybrominated diphenyl ethers by dissolved organic matter. *Environ. Sci. Technol.* **2009**, *43*, 1379−1385.

(24) Smith, K. E.; Thullner, M.; Wick, L. Y.; Harms, H. Sorption to humic acids enhances polycyclic aromatic hydrocarbon biodegradation. *Environ. Sci. Technol.* **2009**, *43*, 7205−7211.

(25) Visser, A. W.; Kiørboe, T. Plankton motility patterns and encounter rates. *Oecologia* **2006**, *148*, 538−546.
(26) Kiørboe, T.; Grossart, H.-P.; Ploug, H.; Tang, K. Mechanisms and rates of bacterial colonization of sinking aggregates. *Appl. Environ. Microbiol.* **2002**, *68*, 3996−4006.
(27) Kiørboe, T. *A Mechanistic Approach to Plankton Ecology*; Princeton University Press, 2008.
(28) Selander, E.; Jakobsen, H. H.; Lombard, F.; Kiørboe, T. Grazer cues induce stealth behavior in marine dinoflagellates. *Proc. Natl. Acad. Sci. U. S. A.* **2011**, *108*, 4030−4034.
(29) Schwarzenbach, R.; Gschwend, P.; Imboden, D. *Environmental Organic Chemistry*, 2nd ed.; John Wiley and Sons Inc.: New York, 2003.
(30) Zicha, D.; Dunn, G. A.; Brown, A. F. A new direct-viewing chemotaxis chamber. *J. Cell Sci.* **1991**, *99* (Pt 4), 769−775.
(31) Smith, K. E. C.; Oostingh, G. J.; Mayer, P. Passive dosing for producing defined and constant exposure of hydrophobic organic compounds during in vitro toxicity tests. *Chem. Res. Toxicol.* **2010**, *23*, 55−65.
(32) Booij, K.; Smedes, F.; van Weerlee, E. M. Spiking of performance reference compounds in low density polyethylene and silicone passive water samplers. *Chemosphere* **2002**, *46*, 1157−1161.
(33) Muinonen-Martin, A. J.; Veltman, D. M.; Kalna, G.; Insall, R. H. An improved chamber for direct visualisation of chemotaxis. *PLoS One* **2010**, *5*, e15309.
(34) Rusina, T. P.; Smedes, F.; Klanova, J.; Booij, K.; Holoubek, I. Polymer selection for passive sampling: A comparison of critical properties. *Chemosphere* **2007**, *68*, 1344−1351.
(35) Ueda, T.; Kobatake, Y. Hydrophobicity of biosurfaces as shown by chemoreceptive thresholds in *Tetrahymena*, *Physarum* and *Nitella*. *J. Membr. Biol.* **1977**, *34*, 351−368.
(36) Kim, D. H.; Casale, D.; Koehidai, L.; Kim, M. J. Galvanotactic and phototactic control of Tetrahymena pyriformis as a microfluidic workhorse. *Appl. Phys. Lett.* **2009**, *94*, 163901.
(37) Taylor, G. I. Diffusion by continuous movements. *Proc. London Math. Soc.* **1921**, *s2−20*, 196−212.
(38) Birch, H.; Gouliarmou, V.; Lützhøft, H.-C. H.; Mikkelsen, P. S.; Mayer, P. Passive dosing to determine the speciation of hydrophobic organic chemicals in aqueous samples. *Anal. Chem.* **2010**, *82*, 1142−1146.
(39) Gouliarmou, V.; Smith, K. E. C.; de Jonge, L. W.; Mayer, P. Measuring binding and speciation of hydrophobic organic chemicals at controlled freely dissolved concentrations and without phase separation. *Anal. Chem.* **2012**, *84*, 1601−1608.
(40) Furuno, S.; Foss, S.; Wild, E.; Jones, K. C.; Semple, K. T.; Harms, H.; Wick, L. Y. Mycelia promote active transport and spatial dispersion of polycyclic aromatic hydrocarbons. *Environ. Sci. Technol.* **2012**, *46*, 5463−5470.
(41) Schamfuss, S.; Neu, T. R.; van der Meer, J. R.; Tecon, R.; Harms, H.; Wick, L. Y. Impact of mycelia on the accessibility of fluorene to PAH-degrading bacteria. *Environ. Sci. Technol.* **2013**, *47*, 6908−6915.